

# Monitoring Human Wrist Rotation in Three Degrees of Freedom

Fatemeh Abyarjoo<sup>1</sup>, Armando Barreto<sup>1</sup>, Somayeh Abyarjoo<sup>2</sup>, Francisco R. Ortega<sup>1</sup>, Jonathan Cofino<sup>1</sup>

<sup>1</sup> Florida International University, Miami, FL, USA

<sup>2</sup>Mofid University, Qom, Iran.

{fabya001, barretoa, jcofi001, forte007}@fiu.edu

**Abstract**— This paper presents a rotation tracking system using a tri-axis MEMS accelerometer and a tri-axis magnetometer sensor that is placed on the human hand. This system recognizes the human wrist's rotation in the pronation-supination, extension-flexion and ulnar-radial movements. The proposed system also is able to measure the degrees of the rotations.

**Keywords**— *Pronation-supination; extension-flexion; ulnar-radial; accelerometer; rotation; magnetometer component;*

## I. INTRODUCTION

Humans use their hands for tasks which have a high degree of complexity and utility. The wrist's role is critical in most functional operations of the human hand. Some professions require specific characteristics in the wrist movement including precision, smoothness and minimization of overshoot.

Earlier, most human hand movement detections were performed based on the computer vision approach [1]. Emerging Micro-Electro-Mechanical-System (MEMS) sensors with favorable specifications such as light weight, compact size and low energy consumption resolved many limitations present in the computer vision technique. In contrast to the computer vision approach, utilizing the body-mounted MEMS sensors involves less environmental limitations. The inertial sensors are only influenced by user movement and the external parameters such as light conditions and background changes do not interfere with the computations.

The main contribution of the work reported in this paper is to recognize the wrist's rotation with a tri-axis accelerometer and a tri-axis magnetometer, which are attached to the human hand. The wrist can rotate in three dimensions and the proposed system is able to recognize in which axes the rotation took place. The proposed system also is able to distinguish if the rotation is counterclockwise or clockwise (pronation-supination), if the rotation is upward or downward (extension-flexion), and whether the rotation took place to the right or to the left (ulnar-radial).

## II. RELATED STUDIES

Some research has been performed on placement of inertial sensors on different locations of the human body [1], [2]. Generally, the application areas for hand-motion sensing efforts are in the rehabilitation process, diagnosing disorders, sports training and in human-computer interaction. Chernbumroong [3] used an accelerometer to classify five daily living human activities. Sanka [4] used an accelerometer for tracking patients undergoing rehabilitation after a stroke. Burchfield [5] detected abnormal human movements with a wireless accelerometer network.

Some studies have been performed on the wrist joint movements. Rahman [6] utilized a 2D accelerometer capable of measuring two simultaneous angular movements. That system is able to capture either extension-flexion and pronation-supination, or ulnar-radial and pronation-supination simultaneously. Strohmeier [7] used stretch sensors to measure wrist movement. Crossan [8] investigated the wrist rotation in the resting, seated standing and walking positions. Several studies focused on analysis of wrist rotation [9,10], axes of rotation [11], reference frames [12,13], etc. Some studies investigate how wrist motion changes under different conditions [14-16].

## III. BACKGROUND

### A. Accelerometers

An accelerometer is an electro-mechanical sensor that detects the acceleration forces. These forces include the Earth's gravitational force, which is a static force, and also the dynamic forces caused by the accelerometer's movements.

Generally, the MEMS accelerometers consist of a moveable mass with plates that are attached through a mechanical suspension system to a reference frame [17]. The plates represent capacitors. When an external acceleration is applied to the accelerometer, the mass deflects from its position. The deflection of the mass is measured using the capacitive changes. Depending on the number of the accelerometer's axes, different rotational angles can be detected [18].

The three accelerometer's axes are located in an orthogonal coordinate system, such that the X- and Y- axes are in the



horizontal plane with respect to the Earth, and the Z-axis is outwardly perpendicular to this plane. When the accelerometer is not under any external forces, except the Earth's gravitational force, it measures the projection of the Earth's gravity in the three axes. If the accelerometer is located on the horizontal plane without any movement, the X- and Y- axes show zero and the only sensed acceleration presents in the Z-axis equal to  $-1g$ . It shows a negative number because the orientation of the Earth's acceleration and the orientation of the Z-axis are opposite. The rotational angles around the X- and Y- axes can be calculated by utilizing the accelerometer output. If  $A_x$ ,  $A_y$  and  $A_z$  are the calibrated accelerometer outputs, equations (1) and (2) calculate the rotational angles around the X- and Y- axes respectively. The accelerometer is insensitive to the rotation about the Z-axis. To calculate this rotational angle, which is rotation from magnetic North, a magnetometer should be added to the system [7].

$$\alpha = \tan^{-1}\left(\frac{A_y}{\sqrt{A_x^2 + A_z^2}}\right) \quad (1)$$

$$\beta = \tan^{-1}\left(\frac{A_x}{\sqrt{A_y^2 + A_z^2}}\right) \quad (2)$$

### B. Magnetometers

A tri-axis magnetometer detects the Earth's magnetic field and it is not sensitive to device motion acceleration. This field is described by three orthogonal components. In this arrangement, the positive values point northward in the X-axis, eastward in the Y-axis and downward in the Z-axis. The total Earth's field strength is calculated by equation (3).  $H$  is the magnetic vector on the horizontal plane with respect to the Earth.

$$F = \sqrt{X^2 + Y^2 + Z^2} = \sqrt{H^2 + Z^2} \quad (3)$$

The magnetometer provides the heading angle using a known reference, which is the magnetic north. In our previous work [19], a sensor fusion algorithm was implemented to compensate the tilt error for magnetometer. Based on that sensor fusion algorithm, the magnetometer is used in this study to calculate the rotation about the Z-axis.

## IV. DATA ACQUISITION

The raw data were extracted from a tri-axis accelerometer and a tri-axis magnetometer. The raw data needed to be calibrated. The calibration process was applied to the raw measurements to calculate the normalized data. The accelerometer calibration process produces normalized data so that at any position of the sensor equation (4) is true. In this equation,  $Norm_x$ ,  $Norm_y$  and  $Norm_z$  are normalized data in the X-, Y- and Z-axes respectively.

$$1 = \sqrt{Norm_x^2 + Norm_y^2 + Norm_z^2} \quad (4)$$

To eliminate the noise, the accelerometer normalized data were filtered with a Butterworth low pass filter.

## V. QUADRANT ADJUSTMENT

Figure (1-a) depicts the accelerometer's behavior under the influence of a  $360^\circ$  counterclockwise rotation around the X-axis. The experiment was repeated and this time a  $360^\circ$  clockwise rotation was applied to the sensor. The results are presented in Figure (1-b). Comparing Figure (1-a) and (1-b), it is observed that while the Z-axis waves are the same in both the clockwise and counterclockwise rotations, the Y-axis outputs are reverse in clockwise and counterclockwise rotations.

The experiment was repeated to record the accelerometer behavior in  $360^\circ$  clockwise and counterclockwise rotations around the Y-axis. The results are shown in in Figures (2-a) and (2-b) for counterclockwise and clockwise rotations, respectively.

Equations (1) and (2) were used to calculate the rotation around the X- and Y-axes. The inverse tangent function returns the value on the  $[-\frac{\pi}{2}, \frac{\pi}{2}]$  interval, which are located on the Quadrant I and IV. Figure (3-a) depicts the inverse tangent's output for  $360^\circ$  rotation. Noticeable error is evident in the result of the inverse tangent. While the result should have an increasing trend from the zero to  $360^\circ$ , it appears in the range of  $[-90, 90]$ .

To compute the angle throughout the entire  $360^\circ$  rotation, quadrant justification [20] should be applied to the computations. The inverse tangent yields the correct results for Quadrant I and there is no need to justify this quadrant. In Quadrant II, a decreasing trend is seen from  $90^\circ$  to zero, which should be an increasing trend on the interval  $[90^\circ, 180^\circ]$ . By subtracting the inverse tangent results from  $180^\circ$ , the true results are computed for Quadrant II. In Quadrant III, a negative decreasing trend is observed. Subtracting these negative numbers from  $180^\circ$  yields the correct angles, which are between  $180^\circ$  and  $270^\circ$ . Table (1) shows the Quadrant justification for all Quadrants.

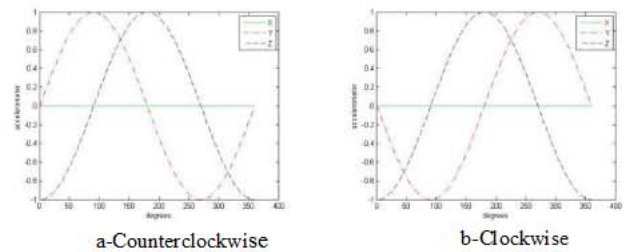


Figure 1: Rotation around the X-axis

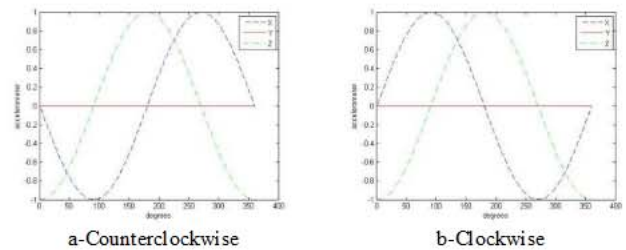


Figure 2: Rotation around the Y-axis



Finally in Quadrant IV, by adding  $360^\circ$  to the negative angles, which are computed from the inverse tangent, the correct results can be computed. Figure (3-b) illustrates the result after applying the quadrant justification.

## VI. WRIST MOVEMENTS

The bones of the human wrist include of eight carpal bones, which are arranged in two rows [21]. The carpal bones connect proximally to the radius of the forearm and distally to the five metacarpals of the hand [22]. The wrist motion occurs by translating and rotating the carpal bones relative to each other and to bones proximal and distal to the wrist.

The International Society of Biomechanics (ISB) has defined anatomical terms of movements [13]. The global motions involving many bones were defined, including wrist flexion-extension and radial-ulnar deviation, as well as forearm pronation-supination movements.

The pronation-supination movements happen when the human wrist rotates, while the palm's direction changes with no variation in the palm-to-arm or thumb-to-arm angles [7]. For the right hand, the counterclockwise motion is defined as pronation, and the clockwise motion is called supination. In pronation, the position of the palm changes from facing sideways to facing down.

The vertical movements of the human wrist are called flexion-extension. The vertical movement of the wrist when it moves upward is called extension and the downward vertical movement is called flexion. In the extension-flexion movements the angle between the palm of the hand and the arm changes.

Figures (4-a) and (4-b) illustrate pronation-supination movements and Figures (5-a) and (5-b) illustrate the extension-flexion movements.

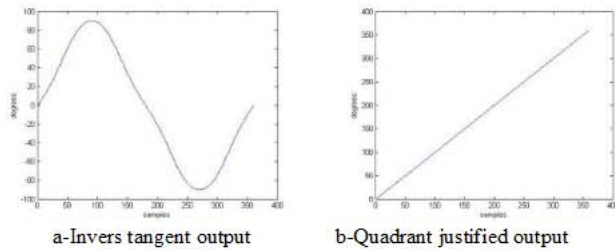


Figure 3: The 360 degrees rotation

Table I. Quadrant Justification

Quadrant	Inverse tangent interval	Correct interval	Quadrant justification
I	$\Theta=[0^\circ, 90^\circ]$	$\Theta=[0^\circ, 90^\circ]$	---
II	$\Theta=[90^\circ, 0^\circ]$	$\Theta=[90^\circ, 180^\circ]$	$180-\Theta$
III	$\Theta=[0^\circ, -90^\circ]$	$\Theta=[180^\circ, 270^\circ]$	$180-\Theta$
IV	$\Theta=[-90^\circ, 0^\circ]$	$\Theta=[270^\circ, 360^\circ]$	$360+\Theta$

The horizontal tilt of the wrist makes the thumb-arm angle change. This movement is called radial when hand rotates to the thumb side and ulnar when the hand rotates to the opposite side [21]. Figure (6) shows the radial-ulnar movements.

The maximum rotation for flexion is  $60^\circ$  and for extension is equal to  $45^\circ$  [6]. The range of maximum motion for pronation and supination together is  $125^\circ$ , with 60% of this range allocated to pronation [6]. For radial and ulnar movements the range of rotation is  $30^\circ$  and  $15^\circ$ , respectively [6].

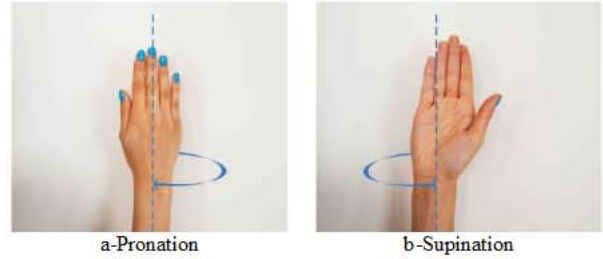


Figure 4: Wrist's Pronation-Supination movements

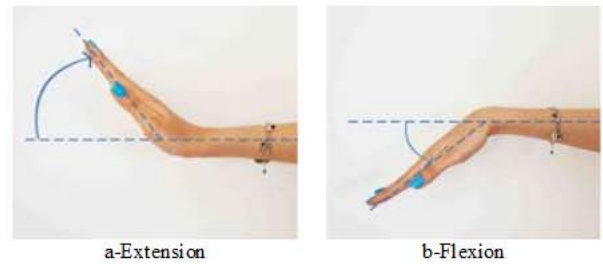


Figure 5: Wrist's Extension-Flexion movements

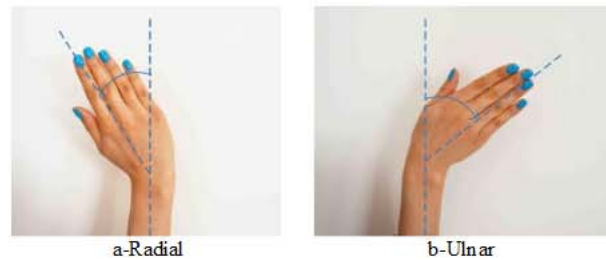


Figure 6: Wrist's Radial-Ulnar movements

## VII. EXPERIMENTAL RESULTS

For evaluating the performance of our proposed approach, different data sets were recorded. The data were recorded from both left and right hands. For all clockwise movements, the system calculates negative angle while in all counterclockwise movements the response of the system is a positive angle.

While the arm was located in the front of the body, supination movement was applied to the right hand. Figure (7) presents the supination rotation results. The experiment was repeated for pronation movement and the result is depicted in Figure (8). Comparing Figures (7) and (8), it is evident that the system delivers negative results for the clockwise movement and positive results for the counterclockwise movements.



Next, extension-flexion movements were applied to the right hand and the results depict in the figures (9) and (10). The system yields negative results for extension and positive results for flexion.

Ulnar-radial movements are rotations around Z-axis. To compute these rotational angles, the magnetometer data are used in combination with the accelerometer data. Ulnar-radial movements were applied to the wrist and experimental results confirmed the performance of the proposed system. For the right hand, radial movement yields a negative rotational angle and ulnar movement produces positive measurement.

To recognize these wrist movements, our proposed system identifies on which axis the rotation was applied and also checks the sign of the measured value.

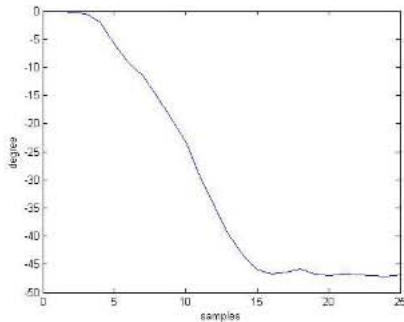


Figure 7: Right hand supination rotation

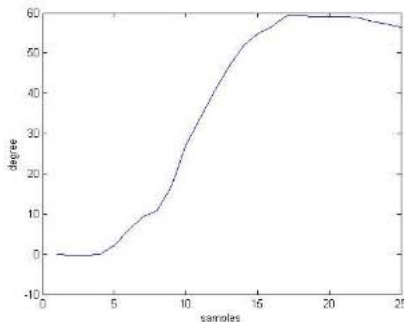


Figure 8: Right hand Pronation rotation

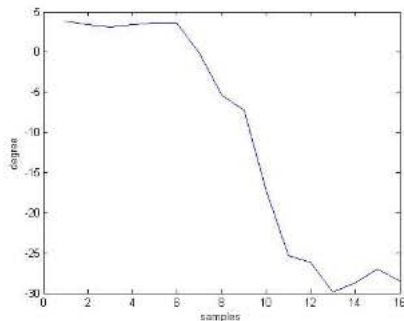


Figure 9: Right hand Extension rotation

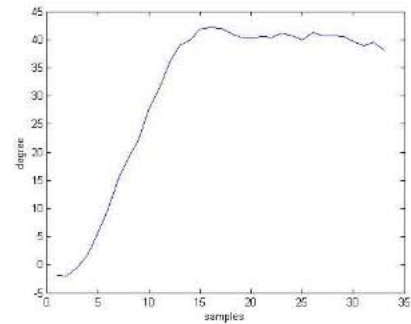


Figure 10: Right hand Flexion rotation

## VIII. CONCLUSION

In this paper, an orientation tracking system was implemented to capture the movement of the human wrist in three degrees of freedom. The proposed system recognizes the type and extent of the rotations. The experimental results confirmed the performance of the system.

## ACKNOWLEDGMENT

This work was sponsored in part by NFS grants HRD-0833093, and CNS-0959985.

## REFERENCES

- [1] Junker, Holger. "Gesture spotting with body-worn inertial sensors to detect user activities." *Pattern Recognition* 41.6 (2008): 2010-2024.
- [2] Zhou, Huiyu, and Huosheng Hu. "Inertial sensors for motion detection of human upper limbs." *Sensor Review* 27.2 (2007): 151-158.
- [3] Chernbumroong, Saisakul, Anthony S. Atkins, and Hongnian Yu. "Activity classification using a single wrist-worn accelerometer." *Software, Knowledge Information, Industrial Management and Applications (SKIMA), 2011 5th International Conference on*. IEEE, 2011.
- [4] Sanka, Sriram. "Utilization of a wrist-mounted accelerometer to count movement repetitions." *Communication Systems and Networks (COMSNETS), 2012 Fourth International Conference on*. IEEE, 2012.
- [5] Burchfield, T. Ryan, and Subbarayan Venkatesan. "Accelerometer-based human abnormal movement detection in wireless sensor networks." *Proceedings of the 1st ACM SIGMOBILE international workshop on Systems and networking support for healthcare and assisted living environments*. ACM, 2007.
- [6] Rahman, Mahfuz. "Tilt techniques: investigating the dexterity of wrist-based input." *Proceedings of the 27th international conference on Human factors in computing systems*. ACM, 2009.
- [7] Strohmeier, Paul, Roel Vertegaal, and Audrey Girouard. "With a flick of the wrist: stretch sensors as lightweight input for mobile devices." *Proceedings of the Sixth International Conference on Tangible, Embedded and Embodied Interaction*. ACM, 2012.
- [8] Crossan, Andrew. "Wrist rotation for interaction in mobile contexts." *Proceedings of the 10th international conference on Human computer interaction with mobile devices and services*. ACM, 2008.
- [9] Youm, Y., and Y. S. Yoon. "Analytical development in investigation of wrist kinematics." *Journal of biomechanics* 12.8 (1979): 613-621.
- [10] Leonard, L.I. "Development of an in-vivo method of wrist joint motion analysis." *Clinical biomechanics (Bristol, Avon)* 20.2 (2005): 166-171.

- [11] Salvia, Patrick. "Analysis of helical axes, pivot and envelope in active wrist circumduction." *Clinical Biomechanics* 15.2 (2000): 103-111.
- [12] Brumbaugh, R. B. "An in-vivo study of normal wrist kinematics." *Journal of biomechanical engineering* 104.3 (1982): 176.
- [13] Wu, Ge, et al. "ISB recommendation on definitions of joint coordinate systems of various joints for the reporting of human joint motion—Part II: shoulder, elbow, wrist and hand." *Journal of biomechanics* 38.5 (2005): 981-992.
- [14] Levin, Mindy F. "Reciprocal and coactivation commands for fast wrist movements." *Experimental brain research* 89.3 (1992): 669-677.
- [15] Valero-Cuevas, F. J., and C. F. Small. "Load dependence in carpal kinematics during wrist flexion in vivo." *Clinical Biomechanics* 12.3 (1997): 154-159.
- [16] Lucidi, C. A., and STEVEN L. Lehman. "Adaptation to fatigue of long duration in human wrist movements." *Journal of Applied Physiology* 73.6 (1992): 2596-2603.
- [17] Andrejašic, Matej. "Mems accelerometers." *University of Ljubljana. Faculty for mathematics and physics, Department of physics, Seminar*. 2008.
- [18] Liao, Wei-Ting. "CORDIC-based inclination sensing algorithm using three-axis accelerometer-based inertial sensors." *Biomedical Engineering and Informatics (BMEI), 2011 4th International Conference on*. Vol. 2. IEEE, 2011.
- [19] Abyarjoo, Barreto, "Implementing a sensor fusion algorithm for 3D orientation detection with inertial/magnetic sensors.", in press.
- [20] Fisher, Christopher J. "Using an Accelerometer for Inclination Sensing." *AN-1057, Application note, Analog Devices* (2010).
- [21] Taylor, Craig L., and Robert J. Schwarz. "The anatomy and mechanics of the human hand." *Artificial limbs* 2.2 (1955): 22-35.
- [22] Charles, Steven Knight. *It's all in the wrist: a quantitative characterization of human wrist control*. Diss. Massachusetts Institute of Technology, 2008.

